JOURNAL OF APPLIED POLYMER SCIENCE VOL. 8, PP. 73-87 (1964)

Geometry Effects and High Speed Tensile Behavior in Styrene Polyblend Systems

J. KENNETH LUND, *Monsanto Chemical Company, Plastics Division, Research Department, Springfield, Massachusetts*

Synopsis

Critical specimen geometry parameters are varied to determine their effect on tensile behavior as a function of rate of testing. Their influence on elongation and energy absorption is pronounced, particularly at low values of specimen cross sectional area and thickness. These effects are attributed to surface imperfections resulting from specimen preparation, and to changes occurring in the combined stress pattern in the specimen. High speed photography and microscope analysis techniques have been developed to determine strain, strain distribution, and strain rate in the specimen gage section during deformation. Elongation measured outside the gage section can be a significant portion of overall specimen deformation; actual strain rate is a fraction of that obtained by assuming all deformation takes place in the gage section. Experimentation is statistically designed and the data statistically analyzed by sequential factorial analysis. Tensile stress response surfaces are accurately predicted by this technique.

INTRODUCTION

The importance of shock resistance or "impact strength" to many end-use material applications needs little introduction. The real problem in studying this property in detail has been one of measurement. Conventional impact test methods suffer from two shortcomings: (*1*) they essentially provide only "one point" data, i.e., deformation rate is not a specified variable, and (*2*) data from these tests cannot be interpreted in terms of both of the fundamental parameters of stress and strain. This is a serious limitation, regarding the possible use of these data by the design engineer. For example, one cannot accurately design a plastic part utilizing Izod impact data. Collectively, all of these tests suffer from the fact that each differs from the others with respect to specimen geometry and applied stress mode.

High speed tensile testing offers solutions to the specific shortcomings mentioned. Rate of testing is variable over a wide range, and stress and strain are measurable simultaneously.

In order, however, to make valid comparisons between data from this test, it is necessary to (*1*) accurately determine strain and strain rate as a function of time, and (*2*) determine the effects of specimen geometry (often times a variable) on stress, strain, and strain rate.

The objectives of this study are twofold: (*1*) to develop accurate techniques for measurement of strain, strain rate, and strain distribution, and (*2*) to evaluate the effects of changing cross-sectional area and width-to-thickness ratio on the tensile properties of dumbbell tensile specimens.

EXPERIMENTAL

An ABS (acrylonitrile–butadiene–styrene: "Lustran 461") polymer and a rubber-modified polystyrene ("Lustrex" HT 88-1) were tested to determine the following tensile properties as a function of strain rate and geometry variables: (*1*) Stress at yield (σ_y) and at failure (σ_f); (*2*) strain at yield (ϵ_y) and at failure (ϵ_f); (*3*) energy absorption to yield (ΔE_y) and to failure (ΔE_f); (*4*) modulus of elasticity.

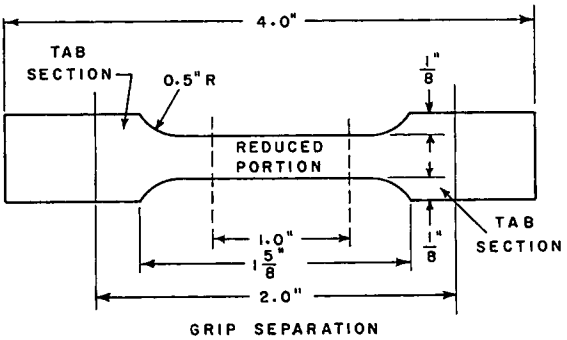

Fig. 1. Tensile specimen.

The experimental program was statistically designed. It is based on Sequential Factorial Analysis[1] which permits an evaluation of the effects of many levels of the independent test parameters while collecting data at a minimum number of experimental conditions.

Rate of crosshead motion on the tester was varied from 60 to 600 to 3000 in./min. Specimen cross-sectional area A was varied from 0.008 to 0.026 to 0.100 square inches. Width-to-thickness ratio W/T was varied from 2.5/1 to 5/1 to 10/1. All testing was done at room temperature. The over-all specimen geometry is shown in Figure 1. Width dimensions depend on particular conditions of A and W/T. Initial grip separation was 2.0 in. in all tests.

Specimens were routed, using a dumbbell-shaped template, from annealed extruded sheet containing no observable orientation.

1. High Speed Tensile Tester

The gas pressurized, hydraulically driven tester used in this study is shown in Figure 2. It was designed by S. Strella of this laboratory, and is a much improved version of the one described in previous study.[2] The test specimen is held by the upper and lower grips at A. It is elongated

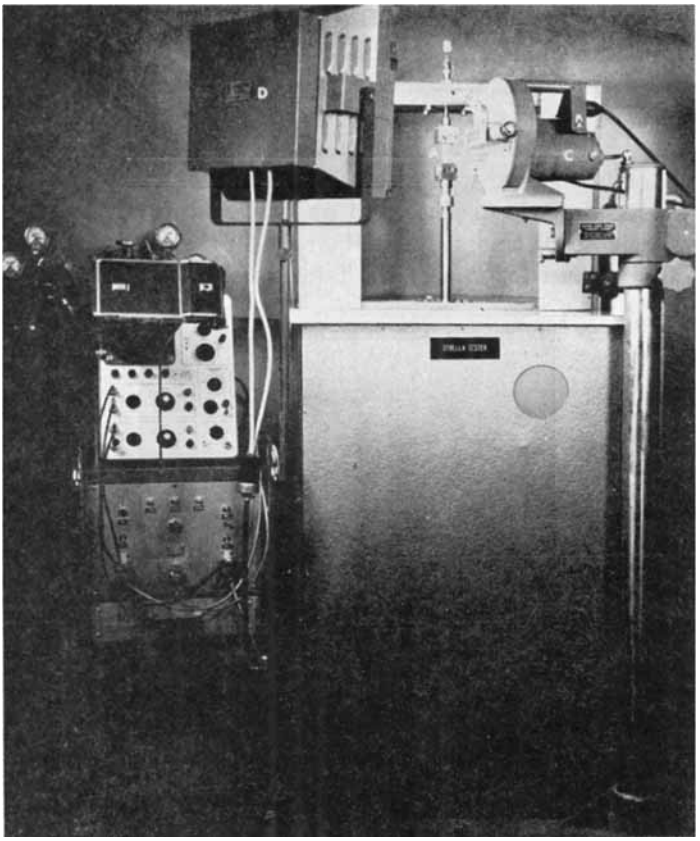

Fig. 2. Gas pressurized, hydraulically driven tester.

to failure by the downward movement of the piston to which the lower grip is attached. Grip faces are diamond-knurl machined to minimize grip slippage. Resultant tensile loads are measured by the force transducer located at *B*. Over-all extension of the specimen (displacement of the lower grip and piston) is measured by a linear potentiometer connected to the bottom of the piston. Load and displacement appear simultaneously on the screen of the oscilloscope, shown to the left of the tester, and are recorded on Polaroid film.

In these tests, the rate of lower grip movement begins at zero velocity and rapidly accelerates to a constant value. The region of acceleration covers approximately the first 0.05 in. of travel.

2. Determination of Strain Properties

In order to study the deformation of these specimens in detail, high speed movie photography was utilized. A uniform pattern of unconnected dots was printed on the front (width) face of the specimens as shown in Figure 3. Printing was accomplished by the spraying of India ink through

a template containing the dot pattern. Testing shows that the pattern remains intact until after fracture of the specimen. Strain is determined by relative changes in the distance between the dots in this pattern during the test.

A Fastax high speed movie camera and lights are shown at C and D in Figure 2. Filming rate was within the range of 3000–4000 frames/sec.

In all tests, the grip displacement at yield and at fail was determined from the oscilloscope traces. Actual strains in the specimen reduced portion were measured for two of the total number of runs at each of the

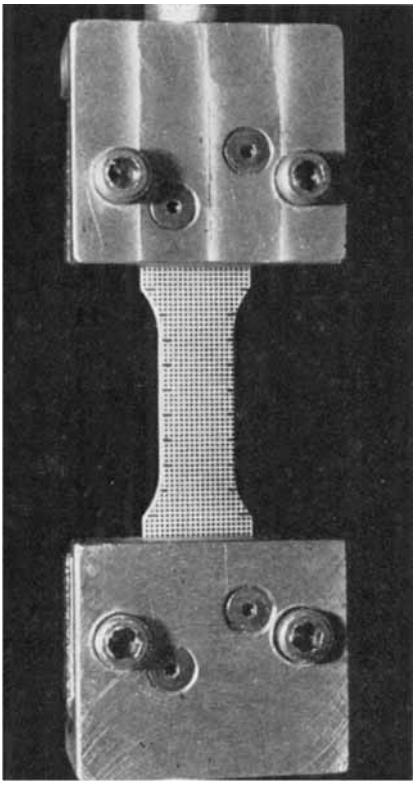

Fig. 3. Uniform pattern of unconnected dots on the front (width) face of the specimens.

experimental conditions investigated. Strain measurement was accomplished by analysis of the developed films with a binocular microscope and graduated eyepiece. In addition, the total elongation between the shoulders of the specimens was measured. Strain in the reduced portion of the unfilmed specimens was determined in the following manner.

The average strain at failure, for example, in the reduced portion is calculated by the following relationship:

$$\epsilon_f = (\Delta l)_s/(L)_{\text{eff}} \tag{1}$$

where $(\Delta l)_s$ is the elongation between the shoulders, and $(L)_{eff}$ is the effective gage length. $(L)_{eff}$ is determined for the filmed runs by measurement of ϵ_f and $(\Delta l)_s$. It does not vary to a great degree with the ranges of geometry variables and test rates used in this study. The values of $(L)_{eff}$ obtained from the filmed runs are used directly in calculating ϵ_f for the unfilmed runs.

The quantity $(\Delta l)_s$ for the unfilmed runs is given by the following relationship:

$$(\Delta l)_s = (\Delta l)_f - (\text{Tab Error}) \tag{2}$$

where $(\Delta l)_f$ is the grip displacement at fail recorded on the oscilloscope, and (Tab Error) is the sum of elongation in the tab section and grip slippage. Tab Error is estimated by using a correlation obtained from the results

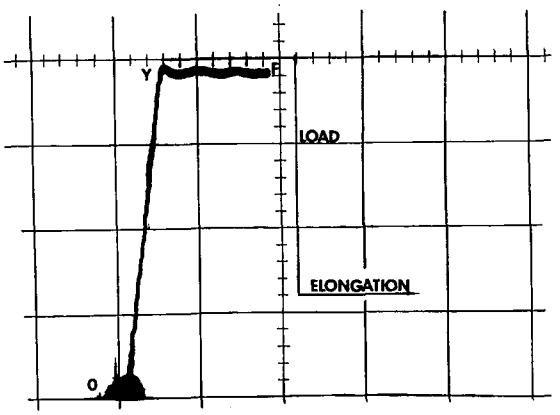

Fig. 4. Oscilloscope recording of specimen load–elongation.

of the filmed runs. The measured tab error in these runs can be correlated with the quantity $(P/W) \cdot (\Delta l)_f$, where P is the tensile load and W is the width of the tab section. For the materials studied, P exhibits almost a flat response from yield to fail, as shown in Figure 4. The average P from yield to fail is used in this correlation.

In order to check the applicability of the correlation, strains for the filmed runs were calculated using it, and compared with the optically measured strains. They differ by an average of ± 1.2 strain percent.

The rate of straining in the reduced portion $\dot{\epsilon}$ is calculated in the following manner. Rate of grip displacement R is approximately constant (true after the initial nonlinearity in rate, which in these tests covers a small portion of the total specimen elongation). At strains near the fail point, $\dot{\epsilon}$ is equal to:

$$\dot{\epsilon} = \epsilon/t = \frac{(\Delta l)_s/(L)_{eff}}{t} \tag{3}$$

where

$$t = (\Delta l)/R \tag{4}$$

and (Δl) is the grip displacement recorded on the oscilloscope. The rate R is set by adjustment of the test equipment. The remaining quantities are determined as previously described.

Discussion

The materials studied do not exhibit any significant degree of strain hardening or cold drawing at the strain rates investigated. Stresses at failure are approximately 5% less than the yield stresses in all specimens tested. It was therefore decided to study only the effects of experimental variables on the yield stress.

The accurate determination of yield strains is a difficult task. Strains of only several percent are involved. The total elongation of the specimen reduced portion at yield is only slightly greater than the experimental error involved in the measurement. Consequently, the measurement of yield strain and elastic modulus is accompanied by sufficient scatter to obscure the effects of the experimental variables. Stress and strain measurements at failure are not similarly affected.

The effects of A and W/T on yield stress are shown in Figure 5. Their effects are minimal. These data are indicative of the stress behavior at all strain rates investigated.

The effect of strain rate on yield stress is shown in Figure 6. This behavior is characteristic of viscoelastic materials.[2,3] As the rate of straining increases, the polymer behaves more like an elastic material. Various

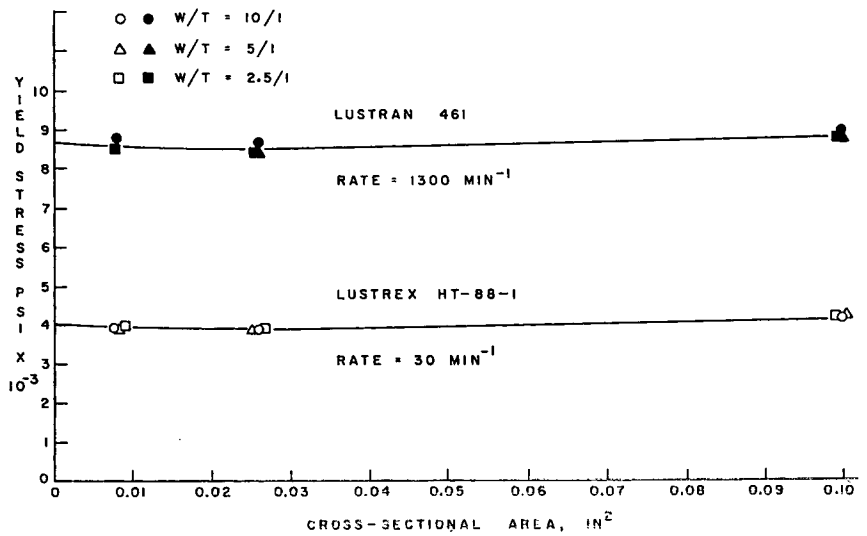

Fig. 5. Effects of A and W T on yield stress.

molecular chain configurations are able to sustain higher stresses before they relax and chain-chain slippage and yielding occur.

Although specimen geometry parameters have an apparently negligible effect on yield properties, variations in A and specimen thickness do produce

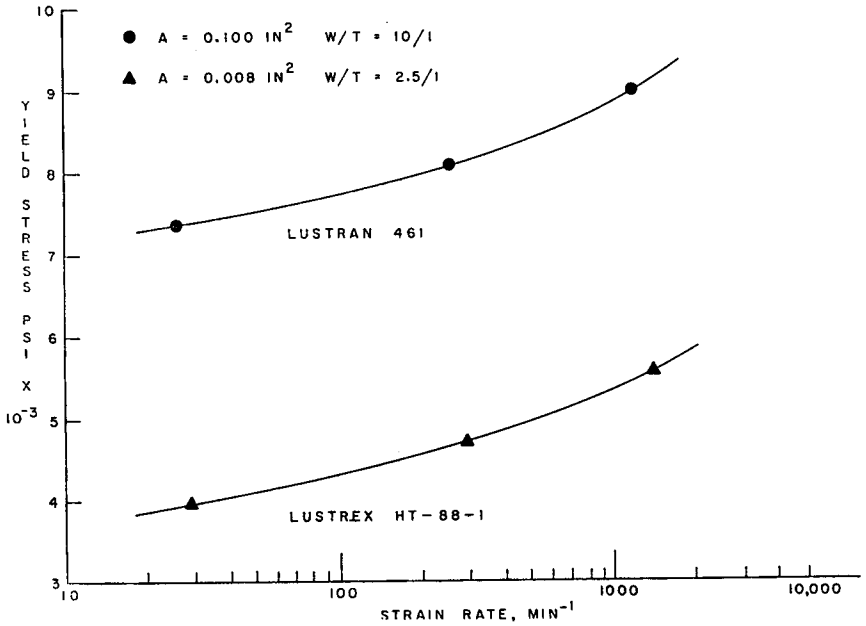

Fig. 6. Effect of strain rate on yield stress.

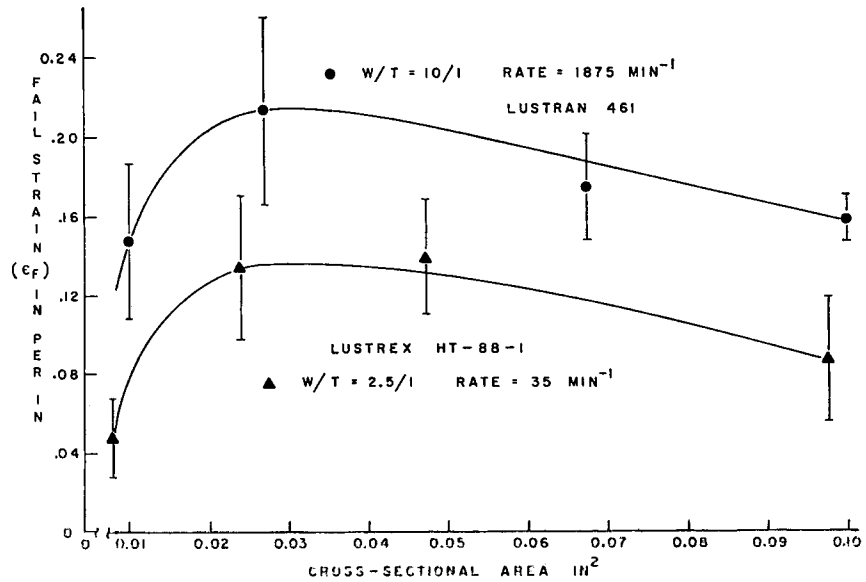

Figure 7.

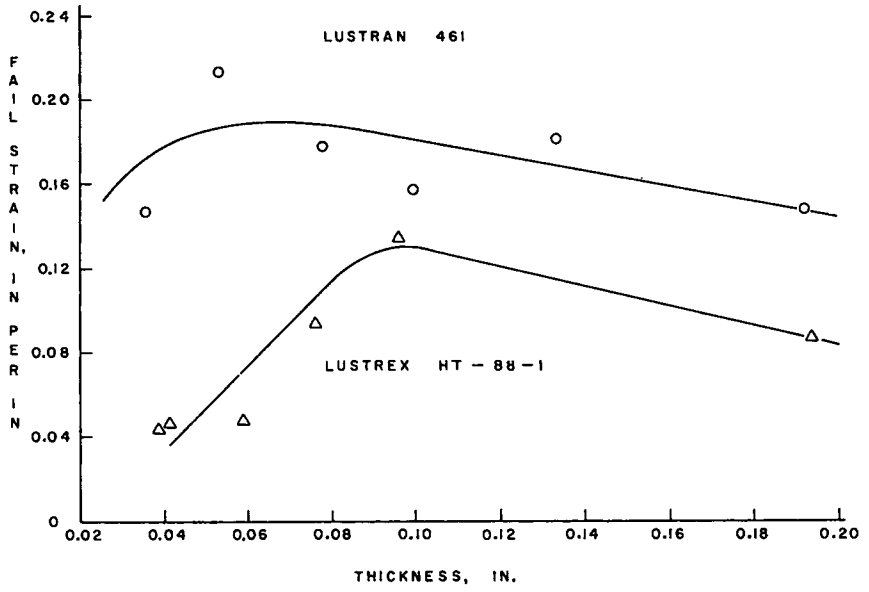

Figure 8.

significant changes in the elongation to failure of these materials. These results are shown in Figures 7 and 8.

Fail strain ϵ_f increases sharply, goes through a maximum, and then begins a gradual decline as either A or thickness is increased. The percentage spread between the smallest and the largest values of ϵ_f is approximately 200% for the rubber-modified polystyrene, and approximately 50% for the ABS material.

Such behavior will be critical in any evaluation of high speed tensile properties where comparisons are made between specimens of varying cross-sectional area or thickness. Valid comparisons between failure properties should be based on the use of a particular value of A or specimen thickness, with little variation about these values.

The rapid decrease in ϵ_f at small values of A has been observed elsewhere.[4] However, its variation at greater values of A and thickness indicates that more than one failure mechanism is operative. At A and thickness values less than those corresponding to the peak ϵ_f position, fracture appears to result due to the stress concentrating effect of machine flaws on the specimen edge (thickness) surfaces. When the values of these parameters are greater than the peak ϵ_f position, it is believed that fracture results from the gradual change of stresses in the specimen to a more complex multiaxial pattern.

Machined surfaces of the specimens have been examined under microscope. Surface roughness of the machined edge is concentrated in the shoulder portions, and in the reduced portion near the intersections of the width and thickness surfaces. Machine marks in the reduced (center)

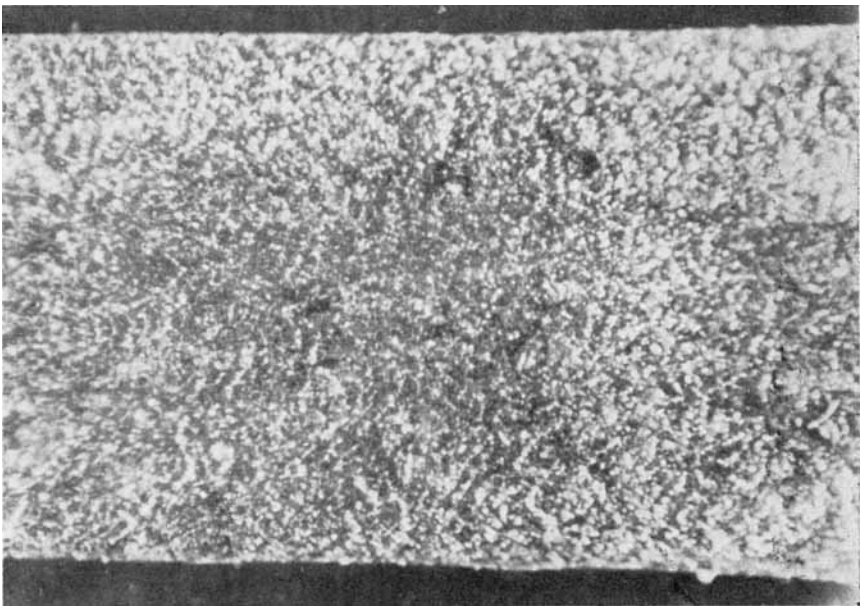

Fig. 9. Machine marks in the reduced (center) portion of a typical specimen.

portion of a typical specimen are shown in Figure 9. These points of stress concentration contribute to the fact that fracture occurs predominantly near the shoulders, and initiates at the edge of the thickness surface. Fracture near the shoulder area is made even more probable because of the stress concentrating effect of the fillet surface.[5]

As the specimen thickness decreases, the flaw effect becomes greater. Initiation of fracture is apparently little influenced by the nominal stress level which is essentially thickness-independent. However, the strain at failure is very much affected. Apparently, a combination of local stress concentration and strain is required to initiate fracture. Consequently, as stress concentration increases with reduced thickness, less strain is required for fracture.

If no other mechanism entered the picture, one would expect ϵ_f to continue rising steadily with increasing A or thickness. This does not occur, and a second mechanism becomes dominant at greater values of these dimensional parameters—a mechanism acting to reduce the strain at failure.

As stated previously, it is believed that this mechanism is the gradual change of stresses in the specimen to a more complex multiaxial pattern as A is increased. Principle stresses, σ_2 and σ_3, in the plane normal to the direction of elongation σ_1 arise in large part from the restraining action of the shoulders and tab sections of the specimen. This restraint acts to prevent the natural lateral contraction of the specimen during elongation. Qualitatively it might appear reasonable that the effects of these restraints arise from (Fig. 10): (*1*) Material in region A which is at a lower longitu-

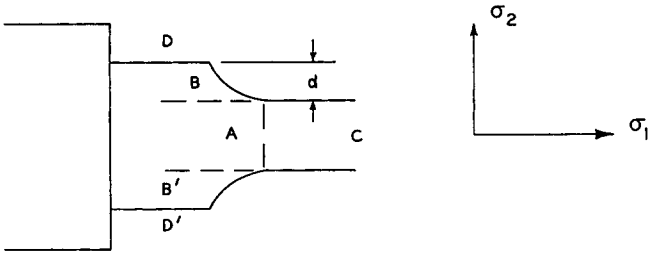

Fig. 10. Restraining action of the shoulders and tab sections of the specimen.

dinal stress than the reduced portion C; it has less tendency to contract laterally and acts as a body in compression in the lateral direction; (*2*) regions B and B' which act as bodies in tension in the lateral direction—due to the lateral restraining action of the grips, acting along the surfaces D and D'.

The width of section C is purposely changed in this study. However, the distance d is a constant, regardless of the specimen width. As the width of C is increased, the absolute magnitude of its natural lateral contraction increases proportionately. Regions B and B' will, therefore, have to distort laterally to a higher degree. This results in an increasing restraint exerted by these portions of the specimen on C. Consequently, σ_2 increases with the width of C.

In the thickness plane of section C, any restraint results in increasing σ_3 and is due primarily to (*1*) the differences in longitudinal stress between the tab section, shoulder, and reduced portion, and (*2*) the absolute magnitude of the natural lateral contraction in the thickness plane. The first

TABLE I
Restraint of Lateral Specimen Contraction

I. W/T ratio held constant, cross-sectional area varied

Values of area	Values of thickness	Thickness restraint effect	Width restraint effect	Over-all restraint effect
Low	Low	Medium	Low	Low-medium
Medium	Medium	Medium	Medium	Medium
High	High	Medium	High	Medium-high

II. Cross-sectional area held constant, W/T ratio varied

Values of W/T	Values of thickness	Values of width	Thickness restraint effect	Width restraint effect	Over-all restraint effect
Low	High	Low	High	Low	Medium
Medium	Medium	Medium	Medium	Medium	Medium
High	Low	High	Low	High	Medium

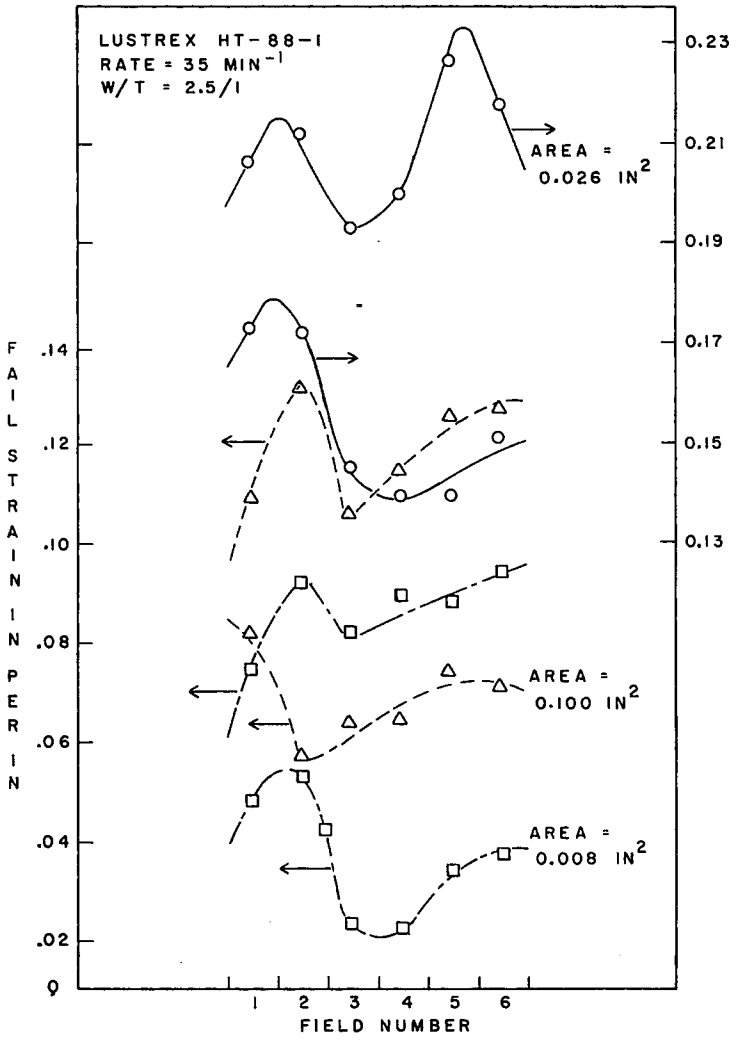

Fig. 11. Strain distributions in the reduced portion of Lustrex HT-88-1.

factor results in increasing restraint with lower specimen width. The latter factor results in increasing restraint with increasing specimen thickness.

The separate and over-all restraint effects are shown in Table I. Area values of Low-Medium-High, for example, refer to qualitatively increasing values of this parameter. The over-all restraint effect is a combination of the thickness and width restraint effects.

Increasing the multiaxiality of the over-all stress pattern results in reduction of the longitudinal strain at failure. This has been most recently shown by Thorkildsen.[6] This reduction in ϵ_f should continue for as long as either or both σ_2 and σ_3 increase with respect to the numerically larger σ_1.

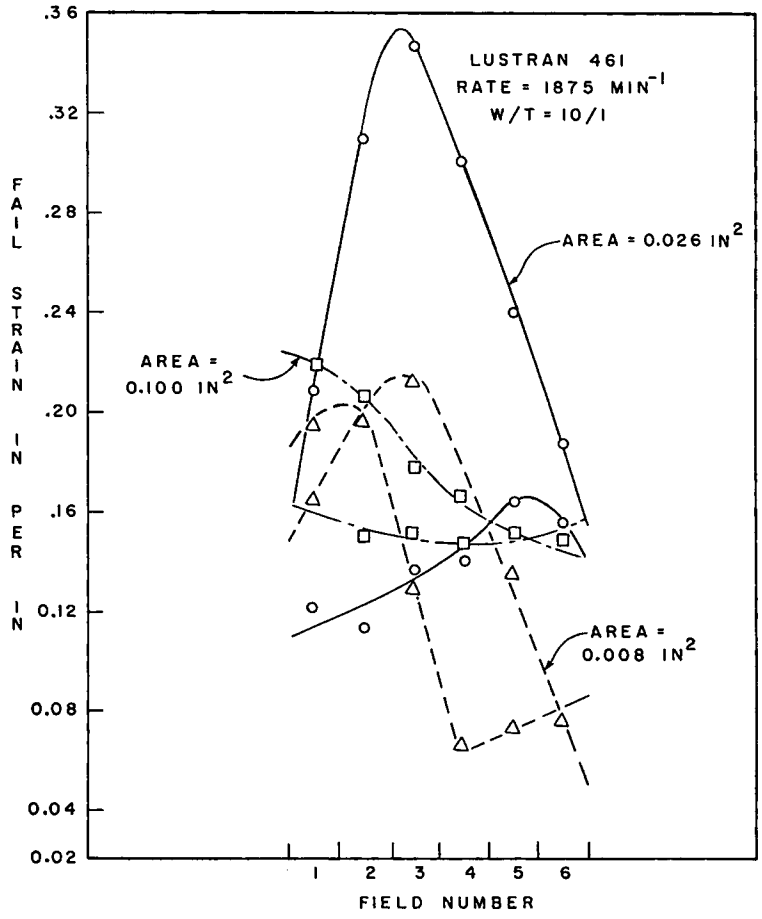

Fig. 12. Strain distributions in the reduced portion of Lustran 461.

The over-all restraint effect shown in Part I of Table I indicates that ϵ_f should decrease with increasing cross-sectional area, which is verified by the data behavior. Part II indicates that ϵ_f should be relatively unaffected by W/T changes. Data confirm this prediction.

Strain distributions in the reduced portion were examined to determine any effect on ϵ_f. These are shown in Figures 11 and 12. The six field numbers correspond to the position of longitudinal strain measurement in the 1.0 in. reduced portion of these specimens, so that

$$\epsilon_f = \sum_{i=1}^{6} \epsilon_i/6 \tag{5}$$

The rubber-modified polystyrene (Lustrex) shows a characteristic unchanging distribution, with only a change in ϵ_f with cross-sectional area. The ABS material (Lustran) does not show a significant difference in

distribution. It does, however, show regions of high deformation. Apparently, the Lustran is able to withstand much higher local strains than the Lustrex without rupturing. These general conclusions dispel primary consideration of a heat buildup phenomenon causing the observed changes in ϵ_f with cross-sectional area.

In addition to the studies just mentioned, an investigation into the fracture mechanics involved in rupturing these two materials has been initiated. Results to date indicate that their fracture mechanisms are significantly different. This work will be part of a future publication.

The significant effect of A on ϵ_f has its counterpart in energy absorption (area under the stress-strain curve) to failure. This is shown in Figure 13.

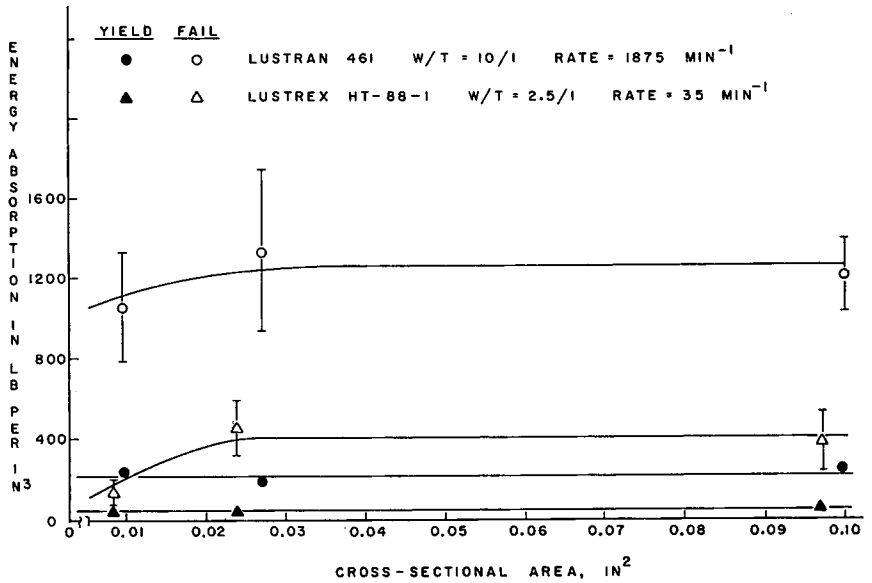

Fig. 13. Energy absorption of Lustran 461 and Lustrex HT-88-1.

Energy absorption ΔE_f is much less affected than ϵ_f, and the effect becomes significant only at very low values of A. The ΔE_f of the ABS is in all cases several times greater than that of the rubber-modified polystyrene. This results from a combination of greater stresses and strains developed in the first material.

The importance of accurate strain and strain rate measurement in any study of this nature cannot be overemphasized. Large differences in the value of ϵ_f can occur if gross assumptions are made in its calculation, rather than making an accurate determination. In Figure 14, ϵ_f is plotted as a function of strain rate. Curves A and B represent ϵ_f, calculated by assuming that all elongation takes place in the 1.0 in. reduced portion of the specimen. Curves A' and B' are obtained by the technique described in the Experimental section. The slopes of these curves remain approxi-

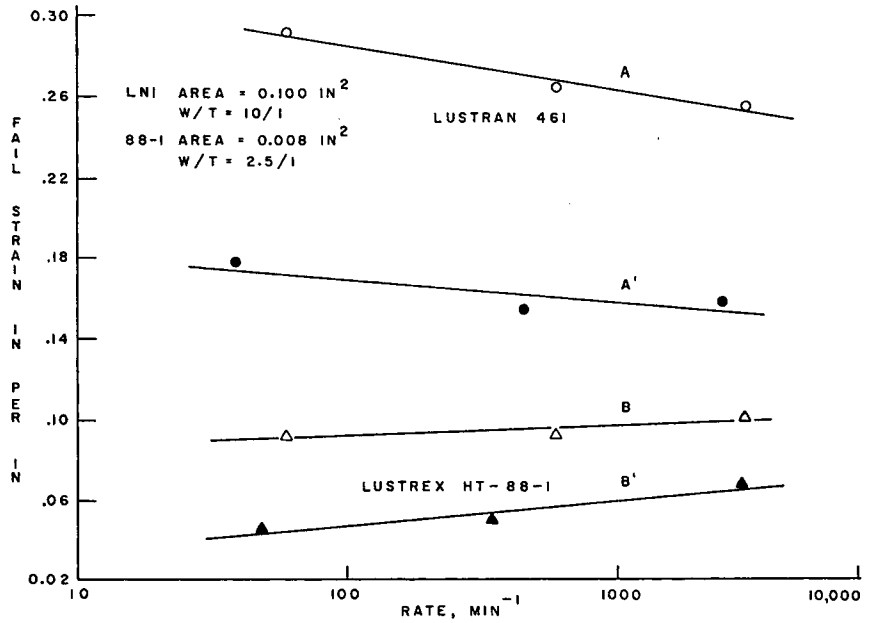

Fig. 14. Strain rate of Lustran 461 and Lustrex HT-88-1.

mately the same. However, making the assumption leading to curves A and B can result in an over-estimate of up to 100% in ϵ_f determination.

Similarly, there are large differences between the crosshead rate and strain rate, as determined in the Experimental section. This is shown in Table II. For many polymeric materials, there are critical strain rates at which ϵ_f changes drastically.[7] Consequently, it is important to determine $\dot{\epsilon}$ with accuracy.

TABLE II
Comparison of Crosshead and Strain Rates

	Lustran 461			Lustrex HT 88-1		
Crosshead rate (R), in./min.	60	600	3000	60	600	3000
Strain rate ($\dot{\epsilon}$), min.$^{-1}$	40	370	1875	35	345	1900

Conclusions

The accurate measurement of strain and strain rate is a necessity in any detailed study of high speed material behavior. The measurement of relative displacements in a dot pattern printed on the specimen surface has been found to be a worthwhile method for accomplishing this objective.

The elongation of tensile specimens to failure is significantly influenced by specimen cross-sectional area and thickness. These effects are believed

to be due to surface machining flaws and to changes occurring in the multiaxial stress pattern in the specimen.

The author acknowledges with appreciation the helpful discussions with E. C. Harrington, Jr. and F. D. Stockton, and the permission of the Plastics Division of the Monsanto Chemical Company to publish this study.

References

1. Harrington, E. C., Proceedings of ACS Div. of Organic Coatings and Plastics Chemistry, **21**, 22 (1961).
2. Strella, S., *High Speed Testing*, Vol. 1, Interscience, New York, 1960, pp. 27–40.
3. Ely, R. E., *High Speed Testing*, Vol. 1, Interscience, New York, 1960, pp. 3–26.
4. Kula, E. B., and N. H. Fahey, *Mater. Res. Std.*, **1**, 631 (1961).
5. Riggs, N. C., and M. M. Frocht, *Strength of Materials*, Ronald Press, New York, 1938, p. 386.
6. Thorkildsen, R. L., General Electric General Engineering Laboratory Report No. 62GL48, March (1962).
7. Amborski, L. E., and T. D. Mecca, *J. Appl. Polymer Sci.*, **4**, 332 (1960).

Résumé

Les paramètres géométriques du spécimen critique ont été modifiée en vue de déterminer leur effet sur le comportement à la tension en fonction de la vitesse d'essai. Leur influence sur l'élongation et l'absorption d'énergie est importante, particulièrement aux faibles valeurs de la surface de la section transversale du spécimen et aux faibles épaisseurs. Ces effets ont été attribuées aux imperfections de surface résultant de la préparation du spécimen et aux changements qui ont lieu dans les tensions combinées dans l'échantillon. Les techniques de photographies à vitesse rapide et d'analyse au microscope ont été développées en vue de déterminer la tension, la distribution de la tension et la vitesse de tension dans la section de mesure de l'échantillon pendant la déformation. L'élongation mesurée en dehors de la section de mesure peut être une portion importante de la déformation totale de l'échantillon; la vitesse de tension actuelle et une fraction de celle obtenue en admettant que toutes les déformations ont lieu dans la section de mesure. L'expérimentation est effectuée statistiquement et les résultats analysés d'une façon statistique par l'analyse factorielle en série. Les surfaces de réponse à la tension d'élongation sont prévues d'une façon précise par cette technique.

Zusammenfassung

Die kritischen Parameter für die Geometrie der Probe werden variiert, um ihren Einfluss auf das Zugverhalten als Funktion der Testgeschwindigkeit zu bestimmen. Ihr Einfluss auf die Dehnung und Energieabsorption tritt besonders bei niedrigen Werten von Probenquerschnitt und Dicke in Erscheinung. Diese Einflüsse werden auf herstellungsbedingte Oberflächenfehlstellen und auf Veränderungen im kombinierten Spannungsdiagramm der Probe zurückgeführt. Eine Kurzzeitphotographiertechnik und ein mikroskopisches Analyseverfahren wurden zur Bestimmung der Spannung, der Spannungsverteilung und der Spannungsgeschwindigkeit im Probenmessquerschnitt während der Verformung entwickelt. Die ausserhalb des Messquerschnitts gemessene Dehnung kann einen westentlichen Teil der Gesamtverformung der Probe bilden, die tatsächliche Verformungsgeschwindigkeit ist nur ein Bruchteil der unter der Annahme erhaltenen, dass die gesamte Deformation im Messquerschnitt stattfindet. Die Versuchsdurchsführung wird statistisch geplant und die Ergebnisse durch eine Sequenz-Faktoren-Analyse statistisch ausgewertet. Die Flächen für das Zugspannungsverhalten können nach diesem Verfahren genau vorausgesagt werden.